



Published in final edited form as:

Pharmacol Res. 2023 August ; 194: 106851. doi:10.1016/j.phrs.2023.106851.

A novel *HIF2A* mutation causes dyslipidemia and promotes hepatic lipid accumulation

Feiqiong Gao^{1,4,#}, Qigu Yao^{1,4,#}, Jiaqi Zhu^{1,4}, Wenyi Chen^{1,4}, Xudong Feng^{1,4}, Bing Feng^{1,4}, Jian Wu^{1,4}, Karel Pacak⁶, Jared Rosenblum², Jiong Yu^{*,1,4}, Zhengping Zhuang^{*,2}, Hongcui Cao^{*,1,3,4}, Lanjuan Li^{1,4,5}

¹State Key Laboratory for the Diagnosis and Treatment of Infectious Diseases, Collaborative Innovation Center for Diagnosis and Treatment of Infectious Diseases, The First Affiliated Hospital, Zhejiang University School of Medicine, 79 Qingchun Rd., Hangzhou City 310003, China

²Neuro-Oncology Branch, National Cancer Institute, National Institutes of Health, Building 37 Room 100, 37 Convent Drive, Bethesda, MD 20892, USA

³Key Laboratory of Diagnosis and Treatment of Aging and Physic-chemical Injury Diseases of Zhejiang Province, 79 Qingchun Rd, Hangzhou City 310003, China

⁴National Clinical Research Center for Infectious Diseases, Hangzhou, China

⁵Jinan Microecological Biomedicine Shandong Laboratory, Jinan City 250117, China

* **Corresponding author:** Hongcui Cao, M.D. State Key Laboratory for the Diagnosis and Treatment of Infectious Diseases, The First Affiliated Hospital, Zhejiang University School of Medicine, 79 Qingchun Rd., Hangzhou City 310003, China. Tel: 86-571-87236451; Fax: 86-571-87236459 hccao@zju.edu.cn Zhengping Zhuang, M.D. Neuro-Oncology Branch, National Cancer Institute, National Institutes of Health, Building 37 Room 100, 37 Convent Drive, Bethesda, MD 20892, USA Phone: 240-760-7055, zhengping.zhuang@nih.gov Jiong Yu, Ph.D. State Key Laboratory for the Diagnosis and Treatment of Infectious Diseases, The First Affiliated Hospital, Zhejiang University School of Medicine, 79 Qingchun Rd., Hangzhou City 310003, China. Tel: 86-571-87236759; Fax: 86-571-87236459 yujiong@zju.edu.cn.

#These authors contributed equally to this work.

Author contributions

H Cao, Z Zhuang, J Yu, and F Gao conducted the conception, design, study supervision, and manuscript writing. J Yu, F Gao and Q Yao contributed to clinical data collection, cellular and animal experiments, and data analysis/statistics. Q Yao, J Zhu, and W Chen participated in molecular biology experiments. X Feng, B Feng, and J Wu participated in analysis and interpretation of data. K Pacak and J Rosenblum revised and edited the manuscript critically, and participated in validation. H Cao obtained financial support for this study. L Li contributed to study supervision. All authors reviewed and approved the final manuscript.

Chemical compounds studied in this article: Palmitic Acid (PubChem CID: 985); Oleic Acid (PubChem CID: 445639); Dexamethasone (PubChem CID: 5743); Methanol (PubChem CID: 887); Streptomycin (PubChem CID: 19649); Puromycin (PubChem CID: 439530); Cholesterol (PubChem CID: 5997).

CRediT authorship contribution statement

Feiqiong Gao: Conceptualization; Data curation; Writing - original draft; Investigation; Methodology. Qigu Yao: Data curation; Investigation; Software. Jiaqi Zhu: Investigation. Wenyi Chen: Investigation. Xudong Feng: Data curation. Bing Feng: Data curation. Jian Wu: Data curation. Karel Pacak: Writing - review & editing; Validation. Jared Rosenblum: Writing - review & editing; Validation. Jiong Yu: Conceptualization; Supervision; Data curation; Methodology. Zhengping Zhuang: Conceptualization; Supervision; Writing - review & editing. Hongcui Cao: Conceptualization; Supervision; Writing - review & editing; Funding acquisition. Lanjuan Li: Supervision

Declaration of interests

The authors declare that they have no competing interests.

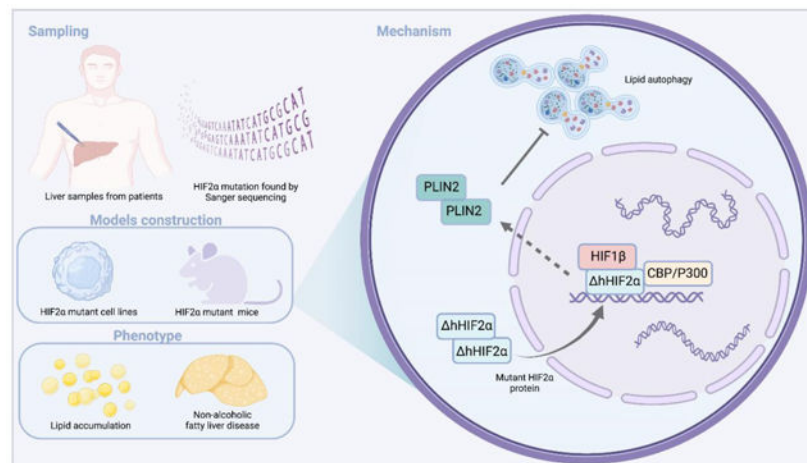
Publisher's Disclaimer: This is a PDF file of an unedited manuscript that has been accepted for publication. As a service to our customers we are providing this early version of the manuscript. The manuscript will undergo copyediting, typesetting, and review of the resulting proof before it is published in its final form. Please note that during the production process errors may be discovered which could affect the content, and all legal disclaimers that apply to the journal pertain.

⁶Section on Medical Neuroendocrinology, Eunice Kennedy Shriver National Institute of Child Health and Human Development, National Institutes of Health, Building 10, Room 1-3140, 10 Center Drive, Bethesda, MD 20892, USA

Abstract

Hypoxia-inducible factor-2 α (HIF-2 α) is a transcription factor responsible for regulating genes related to angiogenesis and metabolism. This study aims to explore the effect of a previously unreported mutation c.C2473T (p.R825S) in the C-terminal transactivation domain (CTAD) of HIF-2 α that we detected in tissue of patients with liver disease. We sequenced available liver and matched blood samples obtained during partial liver resection or liver transplantation performed for clinical indications including hepatocellular carcinoma and liver failure. In tandem, we constructed cell lines and a transgenic mouse model bearing the corresponding identified mutation in HIF-2 α from which we extracted primary hepatocytes. Lipid accumulation was evaluated in these cells and liver tissue from the mouse model using Oil Red O staining and biochemical measurements. We identified a mutation in the CTAD of HIF-2 α (c.C2473T; p.R825S) in 5 of 356 liver samples obtained from patients with hepatopathy and dyslipidemia. We found that introduction of this mutation into the mouse model led to an elevated triglyceride level, lipid droplet accumulation in liver of the mutant mice and in their extracted primary hepatocytes, and increased transcription of genes related to hepatic fatty acid transport and synthesis in the mutant compared to the control groups. In mutant mice and cells, the protein levels of nuclear HIF-2 α and its target perilipin-2 (PLIN2), a lipid droplet-related gene, were also elevated. Decreased lipophagy was observed in mutant groups. Our study defines a subpopulation of dyslipidemia that is caused by this HIF-2 α mutation. This may have implications for personalized treatment.

Graphical abstract



Keywords

Hypoxia-inducible factor-2 α ; Lipid droplet; Perilipin-2; Lipophagy; Non-alcoholic fatty liver; Mutation

1. Introduction

Liver diseases, including hepatitis, cirrhosis, liver cancer, non-alcoholic fatty liver disease (NAFLD), alcohol-related liver disease (ALD) and liver failure, have become some of the top killers worldwide [1, 2]. Dyslipidemia is taken as high triglyceride (TG), high total cholesterol (TC), high low-density lipoprotein cholesterol (LDL-C), high non-high-density lipoprotein cholesterol (non HDL-C), or low HDL-C [3, 4]. These diseases may be due to familial germline inherited mutations or sporadic somatic mutations or other causes including environmental factors or exposures. Constitutional mutations in *ATP7B*, *FAH* and *HFE* have been reported to cause liver cirrhosis [5]. Somatic mutations in *CTNNB1*, *TP53*, *VEGFA* and *ARID1A* have been associated with liver cancer [5]. *VEGFA* expression is regulated by hypoxia signaling through hypoxia-inducible factor (HIF)-2 α (HIF-2 α). Hypoxia also promotes liver cancer by upregulating cytochromes *CYP2S1* and *CYP24A1* [6] and increases hepatic steatosis by adjusting lipid metabolism [7]. This suggests there may be a role of hypoxia signaling pathways, particularly HIF-2 α , and downstream regulated genes in the pathogenesis of some liver diseases.

HIFs are heterodimeric transcription factors first reported by Semenza [8]. The alpha subunit has three isoforms in humans—HIF-1 α , HIF-2 α and HIF-3 α , all of which may dimerize with the beta-subunit (HIF-1 β) [9]. Recently, early mosaicism of mutations in the oxygen-dependent domain (ODD) of HIF-2 α was found to lead to a syndrome of paraganglioma, polycythemia, and somatostatinoma, or Pacak-Zhuang syndrome [10, 11]. Under normal oxygen conditions, the ODD of HIF-2 α , is hydroxylated by prolyl hydroxylase domain-containing protein 2 (PHD2), which leads to ubiquitination of HIF-2 α by von Hippel-Lindau protein, which tags HIF-2 α for subsequent proteosomal degradation. Under hypoxic conditions, the ODD of HIF-2 α is not hydroxylated, resulting in stabilization of HIF-2 α , which allows it to function as a transcription factor [12, 13]. These mutations in the ODD of HIF-2 α similarly prevent hydroxylation of the ODD and lead to pseudo-hypoxia signaling and activation of downstream genes, including those related to lipid metabolism and lipophagy [14], such as through perilipin-2 (PLIN2), which has been reported to have a role in NAFLD [15, 16].

Several studies have reported that mutations in HIF-2 α contribute to disease in solid organs [10, 17, 18]. Together, the relationship of HIF-2 α to the development of solid tumors and lipid metabolism led us to investigate the role of HIF-2 α in pathologies of the liver. Herein, we sequenced liver tissue from patients with liver diseases requiring surgical intervention such as hepatocellular carcinoma and liver failure. We found that a subset of patients had a previously unreported gain-of-function somatic c.C2473T (p.R825S) mutation (hereafter referred to as HIF-2 α ^{mut}) in the C-terminal transactivation domain (CTAD) of HIF-2 α . This domain is hydroxylated by factor inhibiting HIF-1 (FIH-1) in normal oxygen conditions, thereby inhibiting nuclear translocation of HIF-2 α and activation of downstream genes in an oxygen-dependent manner [19, 20]. Thus, to investigate the impact of these mutations on lipid metabolism in liver disease, we generated and evaluated a transgenic mouse model bearing this mutation and primary hepatocytes derived from this model.

2. Materials and methods

2.1. Patient samples and study design

We retrospectively collected liver tissue from patients in The First Affiliated Hospital of Zhejiang University School of Medicine from January 2011 to December 2014. All participants were diagnosed with hepatopathy such as hepatocellular carcinoma and liver failure and had indications for partial liver resection or liver transplantation. These individuals varied in age and gender, without other serious medical conditions. We sequenced these liver samples and available matched blood (n=2) by Sanger sequencing for HIF-2 α mutations. All participants signed written informed consent. And this study was carried out in accordance with Declaration of Helsinki and was approved by the Ethics Committee of The First Affiliated Hospital of Zhejiang University School of Medicine (No. 2014–272).

2.2. Cell culture and treatment

Human cell lines LO2 and HEK293 cells were cultured in DMEM high glucose medium (Gibco, Grand Island, NY, USA) with 10% fetal bovine serum (FBS; Corning, Manassas, VA, USA), 1% streptomycin-penicillin. 786O cells were cultured in RPMI-1640 (BasalMedia, Shanghai, China) with 10% FBS and 1% streptomycin-penicillin. To construct hyperlipidemic cell models, LO2 and HEK293 cells were treated with free fatty acids (FFA, 1mmol/L) containing palmitate and oleate (1:2; Sigma-Aldrich, St. Louis, MO, USA) for 24 hours. LO2 and HEK293 cells were transfected with mutant hHIF-2 α (p.R825S), wild-type (WT) hHIF-2 α , or negative control (NC) lentivirus (Five hundred thousand TU lentivirus per ten thousand LO2 cells; forty thousand TU lentivirus per ten thousand HEK293 cells). Puromycin (2.0 μ g/ml) was used to screen positive cells 48 hours after transfections. The efficacy of transfection was verified through evaluating the expression of HIF-2 α by quantitative Real-Time PCR (qRT-PCR) and the protein levels of flag by western blot.

2.3. Animals and treatment

HIF-2 α ^{mut} mouse was constructed in a mosaic fashion by Cyagen (Guangzhou, China), via previously described gene-targeting techniques [21]. In brief, the HIF2 α ^{mut} vector (Table S1) was constructed and transfected into pluripotent embryonic stem cells (ESCs) of C57BL/6 mice. The ESCs were then microinjected into the blastocyst cavity of C57BL/6 to obtain chimeric mice. Mice with the HIF2 α ^{R825S} homozygous mutation (HIF2 α ^{mut} mice) were attained by several steps of breeding the chimeric mice with wild-type (WT) C57BL/6 mice. Six-to eight-week-old male HIF-2 α ^{mut} and WT C57BL/6 mice were randomly assigned to high-fat diet (HFD) and standard chow diet (SCD) groups, respectively. The HFD group was fed a high-fat diet (60% fat, 20% carbohydrate, 20% protein; Research Diets, New Brunswick, NJ, USA) for 12 weeks to establish a fatty liver mouse model. The SCD group was given standard chow diet for 12 weeks. Hematoxylin and eosin (H&E) and Oil Red O staining were used to confirm the severity of lipid accumulation in the liver.

All animal experimental procedures were conducted according to the Animal Research: Reporting of In Vivo Experiments (ARRIVE) guidelines and a protocol approved by

the Ethics Committee of The First Affiliated Hospital of Zhejiang University School of Medicine (No. 2021–223).

2.4. Isolation and culture of primary hepatocytes

A two-step collagenase perfusion method [22] was employed to isolate primary hepatocytes from HIF-2 α ^{mut} and WT mice. Primary hepatocytes were cultured in William's E (Gibco, Grand Island, NY, USA) supplemented with 10% FBS, 1% streptomycin-penicillin, 40ng/mL dexamethasone, and 1% insulin-transferrin-sodium selenite. To explore the role of lipid droplet-associated protein PLIN2, short interfering RNA (siRNA, 20nmol/L) of PLIN2 and negative control siRNA were used to transfect primary hepatocyte collected from HIF-2 α ^{mut} mice. One day after transfection, we exposed the primary cells to FFA or bull serum albumin (BSA; Sangon Biotech, Shanghai, China) for an additional 24 hours, after which we used them for later biochemical measurements, qRT-PCR or Oil Red O staining.

2.5. Quantitative Real-Time PCR

Trizol reagent (Invitrogen, Carlsbad, CA, USA) was used to extract total RNA from cells and liver samples following manufacturer's protocol. RNA was then converted to cDNA using a two-step RT-PCR kit from Vazyme (Nanjing, China). The levels of mRNA were analyzed with ABI QuantStudio-5 (Applied Biosystems) using SYBR qRT-PCR master mix (Vazyme, Nanjing, China). The primers used are shown in Table S2 and Table S3.

2.6. Western blot

We used radioimmunoprecipitation assay (RIPA) with protease and phosphatase inhibitors (1mmol/L, Beyotime Biotechnology, Shanghai, China) to lyse cells or liver tissue. Nucleoproteins were extracted using a kit from Beyotime Biotechnology (Shanghai, China). We measured protein concentration with a BCA kit (Beyotime Biotechnology, Shanghai, China). After separation by SDS-PAGE gels (GenScript, Nanjing, China), proteins were transferred to polyvinylidene fluoride membranes (Merck-Millipore, Darmstadt, Germany). After being blocked in QuickBlock™ Blocking Buffer for western blot (Beyotime Biotechnology, Shanghai, China) for 30 minutes, membranes were sequentially incubated with the corresponding primary antibodies at 4 degrees overnight, and later with corresponding secondary antibodies for an hour at room temperature. Finally, we exposed the membranes to a chemiluminescent liquid (Thermo Fisher, Rockford, IL, USA). Antibodies used were listed in Table S4.

2.7. Immunohistochemistry and co-immunoprecipitation (Co-IP)

Formalin-fixed mouse liver tissue was stained with H&E after paraffin being embedded and sectioned into 3 μ m. To determine fat deposition, mouse liver cryosections and primary hepatocytes were stained with Oil Red O using a chemical kit from Jiancheng Biotechnology Institute (Nanjing, China). Immunohistochemical analysis of HIF-2 α was performed on paraffin-embedded liver sections using an anti-HIF-2 α primary antibody (1:100, Santa Cruz Biotechnology, Oregon, USA) at 4 degrees overnight and a corresponding secondary antibody (rabbit anti-mouse IgG H&L (HRP), 1:500, Abcam, Cambridge, MA, USA) for one hour at 37 degrees. As for CO-IP, the assay was performed

using a co-immunoprecipitation kit (Thermo Fisher, Rockford, IL, USA) following the recommended methods.

2.8. Biochemical measurements

TG, TC, LDL-C, alanine aminotransferase (ALT), aspartate aminotransferase (AST), intrahepatic TG, TC, and intracellular biochemical indicators were all detected by the corresponding detection kits brought from Jiancheng Biotechnology Institute (Nanjing, China), and were tested according to the recommended protocols.

2.9. Lipidomics analysis

We mixed mouse liver tissue with steel balls and lipid extracts which contain methanol, tert-butyl methyl ether and standard mixtures, followed by homogenization. Supernatant was collected after centrifugation. Next, the supernatant was concentrated and redissolved in mobile phase B. The resultant dissolving solution was analyzed by Ultra Performance Liquid Chromatography (UPLC, ExionLC AD, <https://sciex.com.cn/>) and Tandem mass spectrometry (MS/MS QTRAP®, <https://sciex.com.cn/>). The qualitative and quantitative analyses of metabolites were carried out on Analyst 1.6.3 software (Sciex). We compared differential lipid metabolites by R software (www.r-project.org).

2.10. Statistical analysis

Prism 8 (Graphpad Software, LLC) for macOS was used to analyze the data. Differences between groups were determined by 2-tailed unpaired student's t test (comparisons between two groups) or ANOVA (comparisons among three groups or more), and reported as mean \pm SEM. $P < 0.05$ was defined as statistically significant.

3. Results

3.1. A subset of patients with dyslipidemia have a somatic mutation in the CTAD of HIF-2 α

We sequenced liver tissue from 356 patients diagnosed with liver disease such as hepatocellular carcinoma and liver failure requiring partial liver resection or liver transplantation (Fig. 1A). The characteristics of these 356 patients were shown in Table S5. We found a C to T substitution at base 2473 in exon 16 of the *HIF2A* gene (p.R825S) in the 5 of these patients' liver samples (Fig. 1B, Fig. S1). However, we did not find this mutation in the blood samples of the 5 patients. This location is within the CTAD of HIF-2 α protein, which we found is highly conserved among different species (Fig. 1C). All 5 of these patients had dyslipidemia; the body mass index (BMI) of 4 of these patients was normal while the BMI of 1 patient exceeded the upper limit of normal (Table S6). Of the 351 patients without the mutation, 40 had dyslipidemia, while the whole 5 patients with the mutation have dyslipidemia. Fisher's precision probability test was used to compare the statistic difference in dyslipidemia between patients with and without the mutation. The results showed that patients with the mutation were prone to dyslipidemia ($P < 0.001$). After surgery, the lipid profile remained abnormal in the patients who underwent partial hepatectomy (patients 1–3); however, the high-density lipoprotein cholesterol (HDL-

C) returned to normal in patients who underwent liver transplantation (patients 4 and 5). Supplementary information of the patients with mutation is provided in Table S7.

3.2. HIF-2 α ^{mut} causes fatty liver and weight gain in mice

We found that lipid droplet deposition, which we evaluated by hematoxylin and eosin (H&E) and Oil Red O staining of liver sections from the transgenic mouse model in which we introduced the HIF-2 α ^{mut} in a mosaic fashion (Fig. 2A), which was confirmed by polymerase chain reaction, as compared to the wild-type mice (Fig. S2). Further, the mutation exacerbated the severity of fatty liver induced by a HFD (Fig. 2B, C). HIF-2 α ^{mut} mice treated with SCD or HFD developed fatty liver features with heavier liver weight (Fig. 2D, E). In addition, body weight and liver-to-body weight ratio levels were higher in HIF-2 α ^{mut} mice than in WT mice regardless of whether they were fed HFD or SCD (Fig. 2E), suggesting that the mutation may cause obesity in addition to fatty liver. Despite these differences, in the four groups, the results of liver enzyme tests showed similar ALT and AST levels (Fig. 2F); and no obvious inflammatory response in the liver was found (Fig. S3). However, we found that lipid deposition was increased in primary hepatocytes isolated from the mutant mice as compared to those isolated from WT mice; the mutant primary hepatocytes also showed increased lipid deposition when exposed to the FFA (Fig. 2G).

3.3. HIF-2 α ^{mut} was associated with lipid metabolism in mice

Lipidomic evaluation of the livers of the mouse model also confirmed increased lipid deposition in the mutant compared to the WT mice. The OPLS-DA plot exhibited clear clustering between WT and HIF-2 α ^{mut} mice fed SCD (Fig. 3A). The permutation test of the OPLS-DA model indicated that the model had good predictive power (Fig. 3B). The heatmap of the two groups of mice showed that the livers of mutant mice deposited more lipids, including TG, glyceride (GL), fatty acyl (FA) and sterol (ST), than WT mice (Fig. 3C). According to the fold change, Fig. 3D showed the top 20 differential lipid metabolites detected. TG was found to be the most variable lipid class between the two groups. The relative amount of TG and cholesteryl ester (CE) in the mutant and WT groups were compared in Fig. 3E and F, which shows that TG and CE levels were increased in HIF-2 α ^{mut} mice, which was consistent with the above findings that HIF-2 α ^{mut} mice had increased hepatic lipid droplets (LDs) deposition. KEGG enrichment revealed that the mutation was associated with lipid metabolism-related pathways compared to WT group (Fig. 3G). The lipidomic results of HFD-fed mice are shown in supplementary Fig. S4. There was also an upward trend in lipid content in the mutant group. Interestingly, the differences in lipid metabolites between HIF-2 α ^{mut} and WT mice fed HFD were less pronounced than those between SCD-fed mutant and WT mice, confirming that the mutation itself can affect lipid metabolism. And it also played a role in lipid metabolism in HFD-fed mutant mice.

3.4. HIF-2 α ^{mut} increases fatty acid transport, anabolism, and lipid levels in vivo and in vitro

We found that the transcripts of hepatic fatty acid transport and synthesis-related genes including *Cidea*, *Cd36*, *Fabp2*, *Fabp3* were upregulated in HIF-2 α ^{mut} mice fed HFD or SCD as compared to WT mice (Fig. 4A). We found that serum and hepatic lipid levels in mice

were also influenced by this mutation. After 12-week HFD feeding, serum TC and LDL-C levels were higher in the HIF-2 α ^{mut} group than in WT mice (Fig. 4B). Further, despite a lack of difference in TG levels between the mutant and WT mice, we found that the intrahepatic TG and TC were significantly elevated in the mutant groups as compared to the WT mice (Fig. 4C). Likewise, intracellular TG and the expression of genes responsible for fatty acid transport and anabolism were increased in HIF-2 α ^{mut} primary hepatocytes derived from the livers of the mutant and WT mice regardless of fat content in the growth medium (Fig. 4D and 4E). Notably, TC was higher in the mutant primary hepatocytes cultured only in FFA-free medium.

3.5. Cell lines with HIF-2 α ^{mut} exhibited elevated lipid deposition

We constructed plasmids with WT HIF-2 α and mutant HIF-2 α (Fig. 5A, Table S8, S9), packaged them into lentiviruses, and then transfected the lentiviruses into LO2 and HEK293 cells, respectively. We found that LO2 and HEK293 cells were successfully transfected by assessing HIF-2 α mRNA levels by qRT-PCR and flag protein levels by western blot (Fig. 5B, C). We also found that lipid levels were increased in LO2 and HEK293 cells in which we introduced the mutation compared to those without; however, TC showed an upward trend but did not reach statistical significance (Fig. 5D, E). We found that cells transfected with HIF-2 α ^{mut} exhibited more pronounced lipid accumulation when cultured with FFA-supplemented medium as compared to WT; when both mutant cells and WT cells were cultured in BSA, we did not observe any difference (Fig. 5F and G).

3.6. The mutation increased HIF-2 α protein levels in the nucleus

Although we did not find a difference in the levels of HIF-2 α and HIF-1 α transcripts or protein levels between the four groups of mice, we did find increased nuclear localization of HIF-2 α in fractions extracted from the liver tissue of both mutant and WT mice (Fig. 6A, B). We also observed this in immunohistochemical staining of liver tissues from the mouse model (Fig. 6C). Similarly, while the level of HIF-2 α and HIF-1 α transcripts in primary hepatocytes did not differ between mutant and WT cells as measured by qRT-PCR, target genes of HIF-2 α were markedly upregulated in the mutant cells (Fig. 6D). Likewise, HIF-2 α protein levels did not change in the four groups, but nuclear HIF-2 α protein was increased in HIF-2 α ^{mut} primary hepatocytes (Fig. 6E). In addition, we found that the HEK293 cells with hHIF-2 α lentiviruses also had higher nuclear HIF-2 α protein levels than HEK293 cells with hHIF-2 α and NC lentiviruses in both control and FFA medium (Fig. 6F). Further, co-immunoprecipitation revealed increased amounts of HIF-2 α bound to HIF-1 β in mutant cells compared to WT, suggesting increased transcriptional activity (Fig. 6G).

3.7. Perilipin-2 (PLIN2) protects lipid drops from lipophagy in HIF-2 α ^{mut} groups

We found 112 genes up-regulated and 121 genes down-regulated in HFD-fed HIF-2 α ^{mut} group compared with HFD-fed WT mice through mRNA sequencing of mouse liver tissues and subsequent analysis of differentially expressed genes (Fig. S5). Gene Set Enrichment Analysis (GSEA) revealed that the peroxisome proliferators-activated receptors (PPAR) signaling pathway had an upward trend in the mutant group fed HFD (Fig. S5). After reviewing the literature on HIF-2 α and lipid, we selected the gene PLIN2, a member

of the PPAR signaling pathway, as a target. Then we found that PLIN2 transcripts and protein concentration were both upregulated in the mutant group of mice and their primary hepatocytes (Fig. 7A–C). Further, we found that PLIN2 inhibits lipophagy, thereby reducing lipid deposition. Other lipophagy-related genes were down-regulated (Fig. 7B, C), suggesting that PLIN2 is critical to lipophagy mediated by hypoxia signaling. Later experiments on cell lines also clarified that the mutation elevated the expression of PLIN2 and then downregulated the expression of lipophagy-related genes (Fig. 7D). We determined that the expression of PLIN2 is critical to lipophagy mediated by HIF-2 α , which we used as a model to better understand the downstream effects of hypoxia signaling, by inhibiting expression of PLIN2 in mutant primary hepatocytes with siRNA. When the expression of PLIN2 was inhibited, the expression of lipophagy-related genes was increased (Fig. 7E, F), suggesting that PLIN2 could protect lipid drops from lipophagy. Further, Oil Red O staining showed that PLIN2 inhibition ameliorated LD deposition in mutant primary hepatocytes (Fig. 7G). Based on these findings from our mouse model, we assessed the protein levels of PLIN2 in liver samples from the included patients and confirmed that patients with HIF-2 α ^{mut} (patient 4 and 5) had higher PLIN2 protein levels than those without the mutation (Fig. 7H).

4. Discussion

Herein, we found a subset of patients with dyslipidemia with a previously unreported somatic HIF-2 α mutation. Notably, in 2 of these patients, elevated serum lipid levels returned to normal after liver transplantation. Since HIF-2 α can affect lipid metabolism [23, 24], we suspected that this mutation would be responsible for the dyslipidemia in these patients. Thus, we recapitulated the disease phenotype found in these patients by introducing the corresponding mutation into a transgenic mouse model. Further, we elucidated the mechanism by which abnormal lipid metabolism leading to dyslipidemia occurs in these patients and mice using primary hepatocytes extracted from this model. We found increased nuclear localization of HIF-2 α , which was bound to HIF-1 β , in the mutant group. These findings are consistent with our expectations based on the location of the mutation in the CTAD, which is a domain that regulates nuclear translocation and transactivation of HIF-2 α in response to oxygen [13]. Asparagine residue in CTAD could be hydroxylated by FIH-1 to block the binding of HIF-2 α to CBP/p300 for nuclear translocation, thereby reducing the transactivation activity of HIF-2 α [13]. FIH-1 belongs to the family of dioxygenases whose activity is dependent on oxygen [25]. The gain-of-function mutation may interfere with FIH-induced hydroxylation, and then promote the binding of HIF-2 α to CBP/p300 and HIF-1 β , resulting in increased nuclear translocation of HIF-2 α and its activity as a transcription factor, *i.e.*, increased pseudo-hypoxia signaling.

Patients with dyslipidemia are susceptible to atherosclerosis, stroke and coronary heart disease [26]. Dyslipidemia often accompanies metabolic syndrome and is closely associated with NAFLD, which is the ectopic deposition of lipids in the liver not induced by alcohol. NAFLD, which has been shown to be influenced by chronic changes in altitude, has seen a recent increase in incidence [27]. Nearly 25.24% of people worldwide have NAFLD, ranging from 30.70 to 76.20 years old, yet there continues to be no effective treatment or intervention [28]. NAFLD is also associated with several metabolic syndromes

and increases the risk of cardiovascular diseases [29] and can lead to liver fibrosis and hepatocellular carcinoma [30]. Compared with hepatocellular carcinoma of other etiologies, NAFLD-associated hepatocellular carcinoma has a lower rate of early diagnosis rate and poorer prognosis [31, 32]. Therefore, effective treatment of hyperlipidemia and NAFLD can reduce the incidence of subsequent cardiovascular disease and liver cancer. Identification of the subset of patients with HIF-2 α^{mut} is an opportunity to cure patients with surgery and developed targeted personalized therapeutics. Further, identifying patients whose disease can be cured by surgical intervention, as we have done herein, may lead to a shift in treatment paradigms that could have significant impact on a large population of affected patients.

Aberrant expression of HIF-2 α can lead to a series of pathological conditions by regulating genes responsible for lipid metabolism [33]. However, the effects and pathways vary. Some investigators discovered that hepatic HIF-2 α overexpression increased fatty acid synthesis and caused severe steatohepatitis [7, 34], while others believed that lipid accumulation in the liver was due to impaired fatty acid β -oxidation induced by HIF-2 α rather than upregulation of lipogenic genes [35]. Cen Xie et al. reported that overexpression of intestinal HIF-2 α also resulted in hepatic steatosis by triggering the gene neuraminidase 3 and ceramide levels [36]. Conversely, one study showed that HIF-2 α in adipose tissue helped suppress atherosclerosis by promoting ceramide catabolism [37]. Further, regulation of lipid metabolism by HIF-2 α has implications in other diseases [38]. In renal disease and physiology, several studies have shown that HIF-2 α promotes lipid storage and regulates endoplasmic reticulum homeostasis, thus promoting proliferation of clear cell renal cell carcinoma [39]. In the liver, NAFLD-associated hepatocellular carcinoma has a worse prognosis than those not associated with NAFLD, by upregulating HIF-2 α protein levels [32].

Bo Qiu et al. previously proposed that PLIN2 could be regulated by HIF-2 α to promote lipid storage [39]. Similar to their findings, we found the HIF-2 α^{mut} groups had higher PLIN2 expression and less lipid autophagy. The PLIN family is lipid droplet-related proteins, of which PLIN2 is the most abundant isoform. TG is located inside lipid droplets, while PLIN2 is on the surface serving as a shield [40]. Therefore, PLIN2 can inhibit the degradation of lipids and alter the status of lipid-related diseases. It was reported that PLIN2 could protect lipid drops from lipophagy in the liver and aggravate NAFLD [15, 16], which is consistent with the findings we showed. Autophagy is an important pathway for the removal of waste. And lipophagy is one of the major ways triggering hepatic lipid catabolism [41, 42]. Further exploration in our study showed that inhibition of PLIN2 by siRNA increased lipophagy and attenuated lipid storage in primary hepatocytes caused by HIF-2 α mutation, again supporting our hypothesis. Further, we observed elevated expression levels of genes in regulation of fatty acid transport and synthesis. There may be other pathways for this mutant HIF-2 α to trigger the lipid anabolism, which warrant further exploration.

Herein, we developed a transgenic mouse model that recapitulates the disease of this newly identified subset of patients with liver disease and dyslipidemia due to somatic mutation in HIF-2 α that is potentially curable by surgical intervention. This animal model could serve the greater scientific community in studying these diseases and additional pathways that may warrant further investigation. Diet-induced male C57BL/6 mice are commonly used for in vivo models of NAFLD. However, WT C57BL/6 mice have lower levels of hepatic lipids

and less steatosis than other types of rodents [43, 44]. Compared with the HFD-induced WT C57BL/6 model, HFD-fed HIF-2 α ^{mut} mice exhibit more pronounced TG deposition and vacuolar degeneration in the liver, making up for the deficiencies of WT mice. Our model utilizes targeted gene modification technology to introduce a mosaic mutation that, as our study shows, results in the physiologic alterations consistent with the liver disease found in the patients with this mutation. Therefore, we believe that this model, the HFD-fed male HIF-2 α ^{mut} C57BL/6 mice, may serve as an ideal model to further study NAFLD and other liver diseases related to hypoxia signaling pathways, which will greatly inform our understanding of and ability to treatment these diseases in patients. Our murine NAFLD model was fed a HFD for 12 weeks. The livers of mice developed hepatic steatosis, but no obvious inflammatory cell infiltration or fibrosis was seen. The mouse model we constructed is in the early stage of NAFLD, that is, the NAFL. Levels of serum ALT and AST are not necessarily elevated at this stage [45]. If you want to build a NASH model, you need to fed the mice for a longer time [46].

In conclusion, we identify a mutation in HIF-2 α and find that patients with it are more likely to have dyslipidemia. Our discovery provides an avenue to develop targeted inhibitors for the treatment of this disease that we have found is caused by this mutation. Identification of the subset of patients with HIF-2 α ^{mut} may help to cure patients with surgery and developed targeted personalized therapeutics. Furthermore, our study supplies a novel mouse model of NAFLD for better exploration of the mechanisms of NAFLD.

Supplementary Material

Refer to Web version on PubMed Central for supplementary material.

Acknowledgements

The graphical abstract and Figure 1A were created with BioRender.com.

Funding

This work was supported by Key Research and Development Project of Zhejiang Province (No. 2022C03G2013730), Fundamental Research Funds for the Central Universities (No. 2022ZFH003) and Research Project of Jinan Microecological Biomedicine Shandong Laboratory (No. JNL-2022026C, No. JNL-2023003C).

Data availability

The data for this study are available by contacting the corresponding author upon reasonable request.

Abbreviations:

HIF-2α	Hypoxia-inducible factor-2 α
CTAD	C-terminal transactivation domain
PLIN2	perilipin-2
NAFLD	non-alcoholic fatty liver disease

ALD	alcohol-related liver disease
TG	triglyceride
TC	total cholesterol
LDL-C	low-density lipoprotein cholesterol
non HDL-C	non-high-density lipoproteins
HDL-C	high-density lipoprotein cholesterol
ODD	oxygen-dependent domain
PHD2	prolyl hydroxylase domain-containing protein 2
FIH-1	factor inhibiting HIF-1
FBS	fetal bovine serum
FFA	free fatty acids
WT	wild-type
NC	negative control
qRT-PCR	quantitative Real-Time PCR
ESCs	embryonic stem cells
WT	wild-type
HFD	high-fat diet
SCD	standard chow diet
H&E	hematoxylin and eosin
siRNA	short interfering RNA
BSA	bull serum albumin
RIPA	radioimmunoprecipitation assay
Co-IP	co-immunoprecipitation
ALT	alanine aminotransferase
AST	aspartate aminotransferase
BMI	body mass index
GL	glyceride
FA	atty acyl
ST	sterol

CE	cholesteryl ester
LD	lipid droplet
GSEA	Gene Set Enrichment Analysis
PPAR	peroxisome proliferators-activated receptors

References

- [1]. Xiao J, Wang F, Wong NK, He J, Zhang R, Sun R, Xu Y, Liu Y, Li W, Koike K, He W, You H, Miao Y, Liu X, Meng M, Gao B, Wang H, Li C, Global liver disease burdens and research trends: Analysis from a Chinese perspective, *J Hepatol* 71(1) (2019) 212–221. [PubMed: 30871980]
- [2]. Wang FS, Fan JG, Zhang Z, Gao B, Wang HY, The global burden of liver disease: the major impact of China, *Hepatology* 60(6) (2014) 2099–108. [PubMed: 25164003]
- [3]. Teramoto T, Sasaki J, Ishibashi S, Birou S, Daida H, Dohi S, Egusa G, Hiro T, Hirobe K, Iida M, Kihara S, Kinoshita M, Maruyama C, Ohta T, Okamura T, Yamashita S, Yokode M, Yokote K, Executive summary of the Japan Atherosclerosis Society (JAS) guidelines for the diagnosis and prevention of atherosclerotic cardiovascular diseases in Japan –2012 version, *Journal of atherosclerosis and thrombosis* 20(6) (2013) 517–23. [PubMed: 23665881]
- [4]. Executive Summary of The Third Report of The National Cholesterol Education Program (NCEP) Expert Panel on Detection, Evaluation, And Treatment of High Blood Cholesterol In Adults (Adult Treatment Panel III), *Jama* 285(19) (2001) 2486–97. [PubMed: 11368702]
- [5]. Muller M, Bird TG, Nault JC, The landscape of gene mutations in cirrhosis and hepatocellular carcinoma, *J Hepatol* 72(5) (2020) 990–1002. [PubMed: 32044402]
- [6]. Cabrera-Cano A, Davila-Borja VM, Juarez-Mendez S, Marcial-Quino J, Gomez-Manzo S, Castillo-Rodriguez RA, Hypoxia as a modulator of cytochromes P450: Overexpression of the cytochromes CYP2S1 and CYP24A1 in human liver cancer cells in hypoxia, *Cell Biochem Funct* 39(4) (2021) 478–487. [PubMed: 33377261]
- [7]. Qu A, Taylor M, Xue X, Matsubara T, Metzger D, Chambon P, Gonzalez FJ, Shah YM, Hypoxia-inducible transcription factor 2 α promotes steatohepatitis through augmenting lipid accumulation, inflammation, and fibrosis, *Hepatology* 54(2) (2011) 472–83. [PubMed: 21538443]
- [8]. Wang GL, Jiang BH, Rue EA, Semenza GL, Hypoxia-inducible factor 1 is a basic-helix-loop-helix-PAS heterodimer regulated by cellular O₂ tension, *Proceedings of the National Academy of Sciences of the United States of America* 92(12) (1995) 5510–4. [PubMed: 7539918]
- [9]. Nath B, Levin I, Csak T, Petrasek J, Mueller C, Kodys K, Catalano D, Mandrekar P, Szabo G, Hepatocyte-specific hypoxia-inducible factor-1 α is a determinant of lipid accumulation and liver injury in alcohol-induced steatosis in mice, *Hepatology* 53(5) (2011) 1526–37. [PubMed: 21520168]
- [10]. Zhuang Z, Yang C, Lorenzo F, Merino M, Fojo T, Kebebew E, Popovic V, Stratakis CA, Prchal JT, Pacak K, Somatic HIF2A gain-of-function mutations in paraganglioma with polycythemia, *The New England journal of medicine* 367(10) (2012) 922–30. [PubMed: 22931260]
- [11]. Rosenblum JS, Wang H, Dmitriev PM, Cappadona AJ, Mastorakos P, Xu C, Jha A, Edwards N, Donahue DR, Munasinghe J, Nazari MA, Knutsen RH, Rosenblum BR, Smirniotopoulos JG, Pappo A, Spetzler RF, Vortmeyer A, Gilbert MR, McGavern DB, Chew E, Kozel BA, Heiss JD, Zhuang Z, Pacak K, Developmental vascular malformations in EPAS1 gain-of-function syndrome, *JCI insight* 6(5) (2021).
- [12]. Kaelin WG Jr., Ratcliffe PJ, Oxygen sensing by metazoans: the central role of the HIF hydroxylase pathway, *Molecular cell* 30(4) (2008) 393–402. [PubMed: 18498744]
- [13]. Koh MY, Powis G, Passing the baton: the HIF switch, *Trends in Biochemical Sciences* 37(9) (2012) 364–372. [PubMed: 22818162]
- [14]. Greer SN, Metcalf JL, Wang Y, Ohh M, The updated biology of hypoxia-inducible factor, *The EMBO journal* 31(11) (2012) 2448–60. [PubMed: 22562152]

- [15]. Griffin JD, Bejarano E, Wang XD, Greenberg AS, Integrated Action of Autophagy and Adipose Tissue Triglyceride Lipase Ameliorates Diet-Induced Hepatic Steatosis in Liver-Specific PLIN2 Knockout Mice, *Cells* 10(5) (2021).
- [16]. Tsai TH, Chen E, Li L, Saha P, Lee HJ, Huang LS, Shelness GS, Chan L, Chang BH, The constitutive lipid droplet protein PLIN2 regulates autophagy in liver, *Autophagy* 13(7) (2017) 1130–1144. [PubMed: 28548876]
- [17]. Yang C, Sun MG, Matro J, Huynh TT, Rahimpour S, Prchal JT, Lechan R, Lonser R, Pacak K, Zhuang Z, Novel HIF2A mutations disrupt oxygen sensing, leading to polycythemia, paragangliomas, and somatostatinomas, *Blood* 121(13) (2013) 2563–6. [PubMed: 23361906]
- [18]. Yu J, Shi X, Yang C, Bullova P, Hong CS, Nesvick CL, Dmitriev P, Pacak K, Zhuang Z, Cao H, Li L, A novel germline gain-of-function HIF2A mutation in hepatocellular carcinoma with polycythemia, *Aging* 12(7) (2020) 5781–5791. [PubMed: 32235007]
- [19]. Mahon PC, Hirota K, Semenza GL, FIH-1: a novel protein that interacts with HIF-1 α and VHL to mediate repression of HIF-1 transcriptional activity, *Genes & development* 15(20) (2001) 2675–86. [PubMed: 11641274]
- [20]. Koivunen P, Hirsilä M, Günzler V, Kivirikko KI, Myllyharju J, Catalytic properties of the asparaginyl hydroxylase (FIH) in the oxygen sensing pathway are distinct from those of its prolyl 4-hydroxylases, *The Journal of biological chemistry* 279(11) (2004) 9899–904. [PubMed: 14701857]
- [21]. Bogdan DM, Studholme K, DiBua A, Gordon C, Kanjiya MP, Yu M, Puopolo M, Kaczocha M, FABP5 deletion in nociceptors augments endocannabinoid signaling and suppresses TRPV1 sensitization and inflammatory pain, *Sci Rep* 12(1) (2022) 9241.
- [22]. Papeleu P, Vanhaecke T, Henkens T, Elaut G, Vinken M, Snykers S, Rogiers V, Isolation of rat hepatocytes, *Methods in molecular biology (Clifton, N.J.)* 320 (2006) 229–37.
- [23]. Du W, Zhang L, Brett-Morris A, Aguila B, Kerner J, Hoppel CL, Puchowicz M, Serra D, Herrero L, Rini BI, Campbell S, Welford SM, HIF drives lipid deposition and cancer in ccRCC via repression of fatty acid metabolism, *Nature communications* 8(1) (2017) 1769.
- [24]. Rahtu-Korpela L, Karsikas S, Hörkkö S, Blanco Sequeiros R, Lammintausta E, Mäkelä KA, Herzig KH, Walkinshaw G, Kivirikko KI, Myllyharju J, Serpi R, Koivunen P, HIF prolyl 4-hydroxylase-2 inhibition improves glucose and lipid metabolism and protects against obesity and metabolic dysfunction, *Diabetes* 63(10) (2014) 3324–33. [PubMed: 24789921]
- [25]. Semenza GL, Involvement of oxygen-sensing pathways in physiologic and pathologic erythropoiesis, *Blood* 114(10) (2009) 2015–9.
- [26]. Kopin L, Lowenstein C, Dyslipidemia, *Ann Intern Med* 167(11) (2017) ITC81–ITC96. [PubMed: 29204622]
- [27]. Ruscica M, Zimetti F, Adorni MP, Sirtori CR, Lupo MG, Ferri N, Pharmacological aspects of ANGPTL3 and ANGPTL4 inhibitors: New therapeutic approaches for the treatment of atherogenic dyslipidemia, *Pharmacological research* 153 (2020) 104653. [PubMed: 31931117]
- [28]. Younossi ZM, Koenig AB, Abdelatif D, Fazel Y, Henry L, Wymer M, Global epidemiology of nonalcoholic fatty liver disease-Meta-analytic assessment of prevalence, incidence, and outcomes, *Hepatology* 64(1) (2016) 73–84. [PubMed: 26707365]
- [29]. Gaggini M, Morelli M, Buzzigoli E, DeFronzo RA, Bugianesi E, Gastaldelli A, Non-alcoholic fatty liver disease (NAFLD) and its connection with insulin resistance, dyslipidemia, atherosclerosis and coronary heart disease, *Nutrients* 5(5) (2013) 1544–60. [PubMed: 23666091]
- [30]. Powell EE, Wong VW, Rinella M, Non-alcoholic fatty liver disease, *Lancet (London, England)* 397(10290) (2021) 2212–2224. [PubMed: 33894145]
- [31]. Karim MA, Singal AG, Kum HC, Lee YT, Park S, Rich NE, Nouredin M, Yang JD, Clinical Characteristics and Outcomes of Nonalcoholic Fatty Liver Disease-Associated Hepatocellular Carcinoma in the United States, *Clinical gastroenterology and hepatology : the official clinical practice journal of the American Gastroenterological Association* (2022).
- [32]. Chen J, Chen J, Huang J, Li Z, Gong Y, Zou B, Liu X, Ding L, Li P, Zhu Z, Zhang B, Guo H, Cai C, Li J, HIF-2 α upregulation mediated by hypoxia promotes NAFLD-HCC progression by activating lipid synthesis via the PI3K-AKT-mTOR pathway, *Aging* 11(23) (2019) 10839–10860. [PubMed: 31796646]

- [33]. Mylonis I, Simos G, Paraskeva E, Hypoxia-Inducible Factors and the Regulation of Lipid Metabolism, *Cells* 8(3) (2019) 214. [PubMed: 30832409]
- [34]. Rey E, Meléndez-Rodríguez F, Marañón P, Gil-Valle M, Carrasco AG, Torres-Capelli M, Chávez S, Del Pozo-Maroto E, Rodríguez de Cía J, Aragonés J, García-Monzón C, González-Rodríguez Á, Hypoxia-inducible factor 2 α drives hepatosteatosis through the fatty acid translocase CD36, *Liver international : official journal of the International Association for the Study of the Liver* 40(10) (2020) 2553–2567. [PubMed: 32432822]
- [35]. Rankin EB, Rha J, Selak MA, Unger TL, Keith B, Liu Q, Haase VH, Hypoxia-inducible factor 2 regulates hepatic lipid metabolism, *Mol Cell Biol* 29(16) (2009) 4527–38. [PubMed: 19528226]
- [36]. Xie C, Yagai T, Luo Y, Liang X, Chen T, Wang Q, Sun D, Zhao J, Ramakrishnan SK, Sun L, Jiang C, Xue X, Tian Y, Krausz KW, Patterson AD, Shah YM, Wu Y, Jiang C, Gonzalez FJ, Activation of intestinal hypoxia-inducible factor 2 α during obesity contributes to hepatic steatosis, *Nat Med* 23(11) (2017) 1298–1308. [PubMed: 29035368]
- [37]. Zhang X, Zhang Y, Wang P, Zhang SY, Dong Y, Zeng G, Yan Y, Sun L, Wu Q, Liu H, Liu B, Kong W, Wang X, Jiang C, Adipocyte Hypoxia-Inducible Factor 2 α Suppresses Atherosclerosis by Promoting Adipose Ceramide Catabolism, *Cell Metab* 30(5) (2019) 937–951 e5. [PubMed: 31668872]
- [38]. Gonzalez FJ, Xie C, Jiang C, The role of hypoxia-inducible factors in metabolic diseases, *Nat Rev Endocrinol* 15(1) (2018) 21–32. [PubMed: 30275460]
- [39]. Qiu B, Ackerman D, Sanchez DJ, Li B, Ochocki JD, Grazioli A, Bobrovnikova-Marjon E, Diehl JA, Keith B, Simon MC, HIF2 α -Dependent Lipid Storage Promotes Endoplasmic Reticulum Homeostasis in Clear-Cell Renal Cell Carcinoma, *Cancer Discov* 5(6) (2015) 652–67. [PubMed: 25829424]
- [40]. Conte M, Franceschi C, Sandri M, Salvioli S, Perilipin 2 and Age-Related Metabolic Diseases: A New Perspective, *Trends Endocrinol Metab* 27(12) (2016) 893–903. [PubMed: 27659144]
- [41]. Singh R, Kaushik S, Wang Y, Xiang Y, Novak I, Komatsu M, Tanaka K, Cuervo AM, Czaja MJ, Autophagy regulates lipid metabolism, *Nature* 458(7242) (2009) 1131–5. [PubMed: 19339967]
- [42]. Weidberg H, Shvets E, Elazar Z, Lipophagy: selective catabolism designed for lipids, *Developmental cell* 16(5) (2009) 628–30. [PubMed: 19460339]
- [43]. Kirsch R, Clarkson V, Shephard EG, Marais DA, Jaffer MA, Woodburne VE, Kirsch RE, Hall Pde L, Rodent nutritional model of non-alcoholic steatohepatitis: species, strain and sex difference studies, *Journal of gastroenterology and hepatology* 18(11) (2003) 1272–82. [PubMed: 14535984]
- [44]. Willebrords J, Pereira IV, Maes M, Crespo Yanguas S, Colle I, Van Den Bossche B, Da Silva TC, de Oliveira CP, Andraus W, Alves VA, Cogliati B, Vinken M, Strategies, models and biomarkers in experimental non-alcoholic fatty liver disease research, *Progress in lipid research* 59 (2015) 106–25. [PubMed: 26073454]
- [45]. Rinella ME, Neuschwander-Tetri BA, Siddiqui MS, Abdelmalek MF, Caldwell S, Barb D, Kleiner DE, Loomba R, AASLD Practice Guidance on the clinical assessment and management of nonalcoholic fatty liver disease, *Hepatology* 77(5) (2023) 1797–1835. [PubMed: 36727674]
- [46]. Ito M, Suzuki J, Tsujioka S, Sasaki M, Gomori A, Shirakura T, Hirose H, Ito M, Ishihara A, Iwaasa H, Kanatani A, Longitudinal analysis of murine steatohepatitis model induced by chronic exposure to high-fat diet, *Hepatology research : the official journal of the Japan Society of Hepatology* 37(1) (2007) 50–7. [PubMed: 17300698]

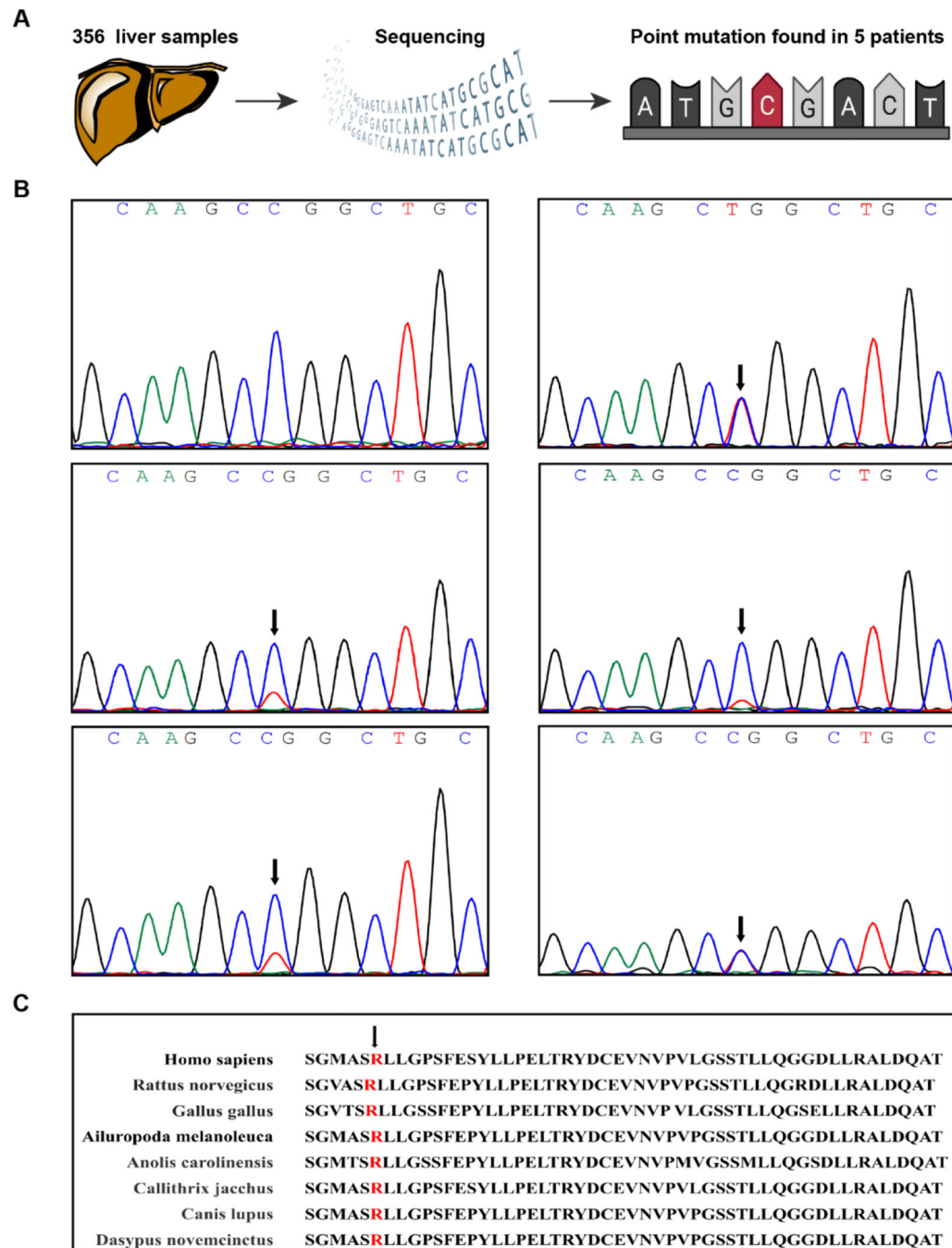


Fig. 1. Sanger sequencing and peptide sequence. (A) 356 liver samples were obtained for Sanger sequencing and a point mutation in *HIF2A* was found in 5 patients. (B) Part of the *HIF2A* gene exon 16 sequencing results in 6 patients. One had no *HIF2A* mutation, while the other five patients carried a C2473T heterozygous mutation in exon 16 of *HIF2A* (arrow). (C) Comparison of polypeptide sequence was conducted. The mutant site was shown to be conserved across species (arrow).

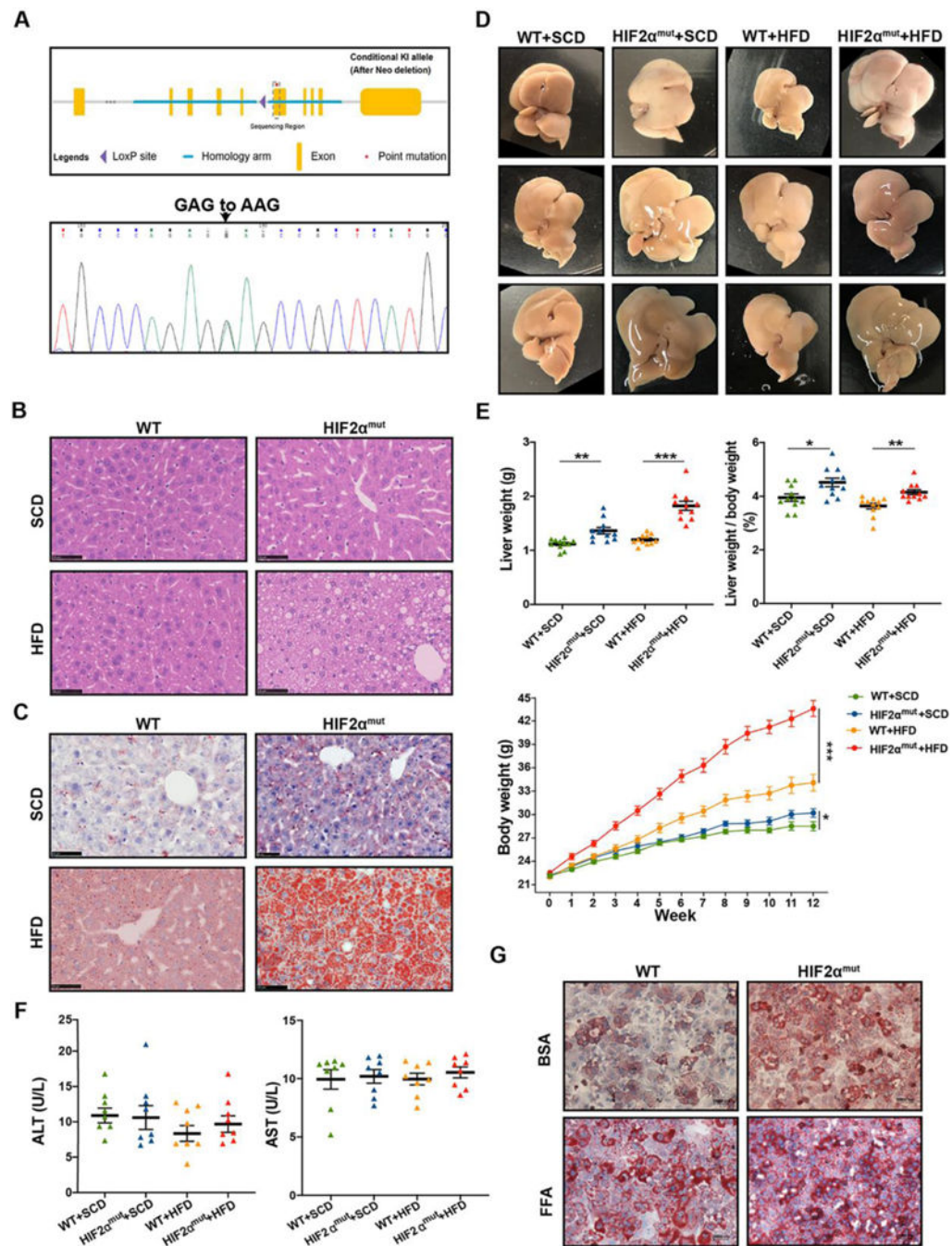


Fig. 2. HIF-2 α^{mut} mice model was established; the mutation resulted in fatty liver and increased body weight in HIF-2 α^{mut} mice. (A) HIF-2 α^{mut} mice were constructed using targeted gene modification technology. (B-D) H&E staining (B), Oil Red O staining (C) and general view (D) of mouse livers. HIF-2 α^{mut} mice and WT mice (control) were fed HFD and SCD, respectively. (E) Liver weight, body weight and liver weight/body weight ratio were compared between HIF-2 α^{mut} and WT mice with different treatments. (F) ALT and AST levels of four groups of mice. (G) Oil Red O staining results of primary hepatocytes.

Primary hepatocytes were isolated from the livers of mutant and WT mice, respectively. The cells were then cultured in the William's E supplemented with BSA or FFA. * $p < 0.05$, ** $p < 0.01$, *** $p < 0.001$. WT: wild-type; HFD: high-fat diet; SCD: standard chow diet; ALT: alanine aminotransferase; AST: aspartate aminotransferase; BSA: bull serum albumin; FFA: free fatty acids.

Author Manuscript

Author Manuscript

Author Manuscript

Author Manuscript

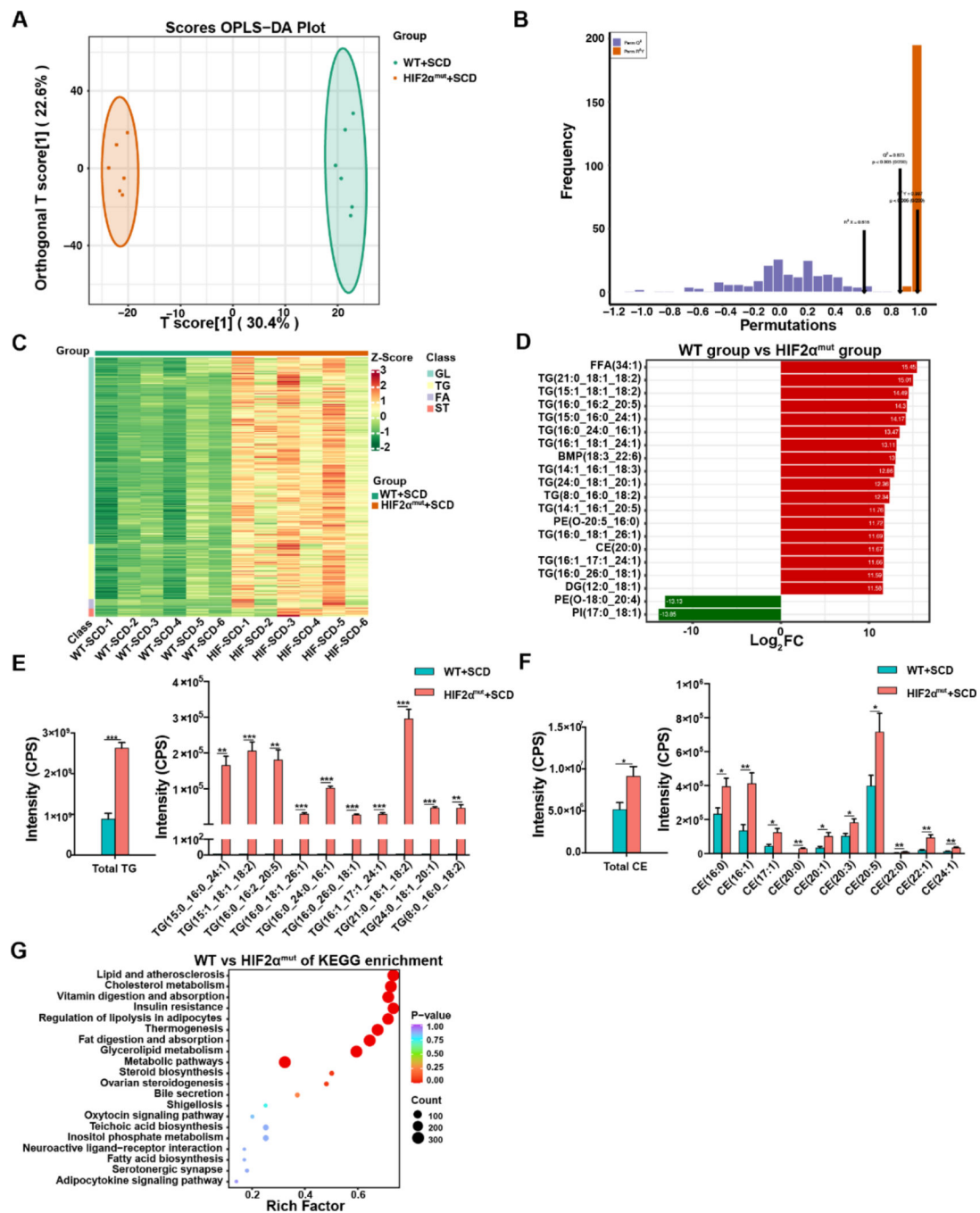


Fig. 3. HIF-2 α^{mut} was associated with lipid metabolism in SCD-fed mice. (A) OPLS-DA model of lipid metabolites in the livers of WT and HIF-2 α^{mut} mice fed SCD. (B) The permutation test of the OPLS-DA model showed that $Q^2=0.873$, $R^2X=0.616$, $R^2Y=0.997$, indicating that the model had good predictive ability. (C) Different classes of lipids were compared between SCD-fed WT and mutant mice by heatmap. The results demonstrated that the liver of mutant mice deposited more lipids than WT mice. (D) The fold change graph showed the top 20 differential lipids in HIF-2 α^{mut} mice compared to WT mice. Red represented up-regulation

of lipid content and green represented down-regulation. (E and F) The relative levels of TG (E) and CE (F) for the two groups were presented as histograms. (G) KEGG pathway analysis of HIF-2 α mutant mice unique to WT group. * $p < 0.05$, ** $p < 0.01$, *** $p < 0.001$. SCD: standard chow diet; WT: wild-type; TG: triglyceride; CE: cholesteryl ester.

Author Manuscript

Author Manuscript

Author Manuscript

Author Manuscript

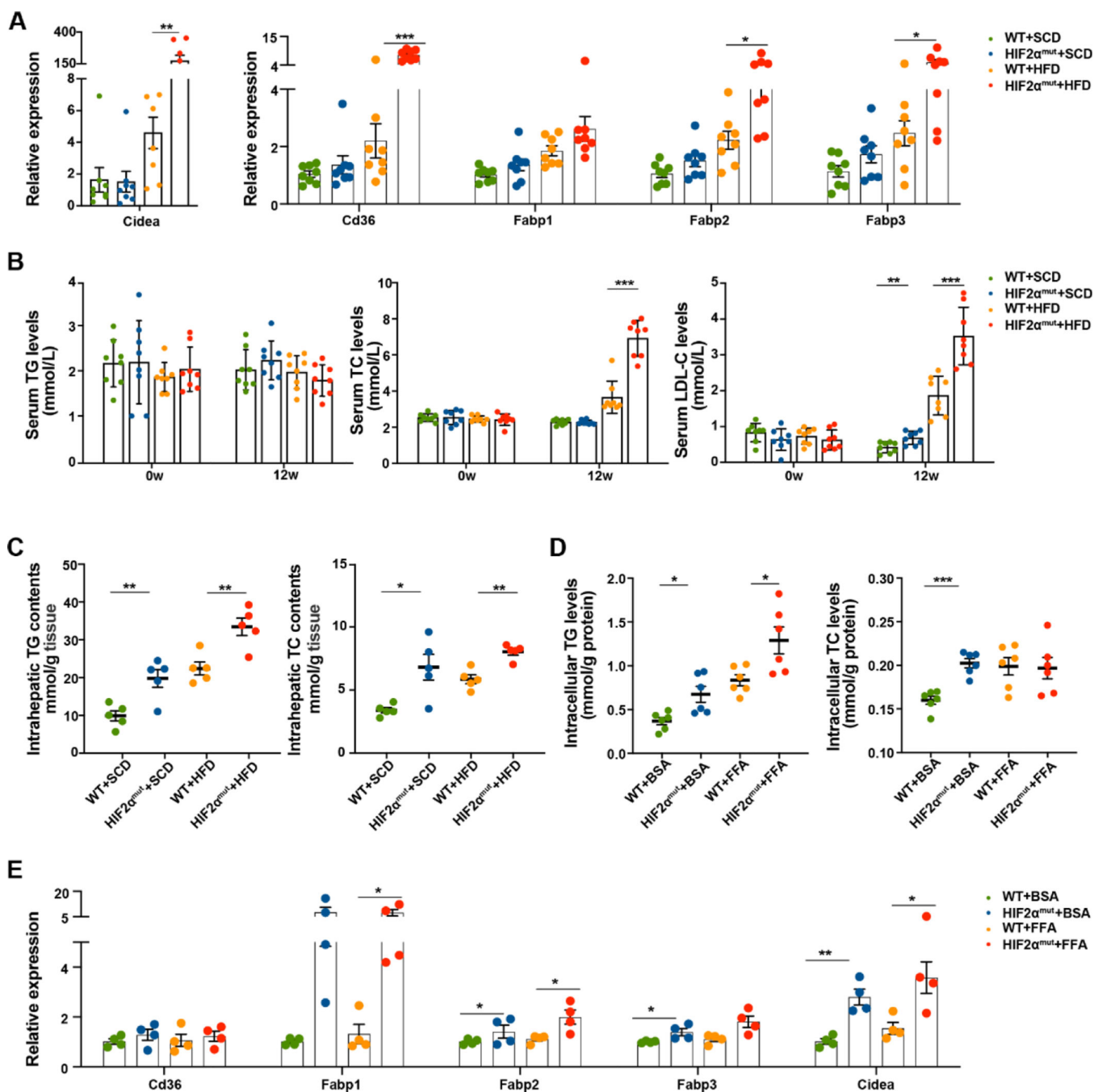


Fig. 4. HIF-2 α^{mut} affected fatty acid transport and synthesis, as well as lipid levels in vivo and in vitro. (A) mRNA levels of genes responsible for fatty acid transport and synthesis in mouse liver were detected by qRT-PCR. (B) Comparison of serum TG, TC and LDL-C in WT and mutant mice with different treatments. (C) Intrahepatic TG and TC levels of the four groups. (D) Intracellular TG and TC levels were tested in the primary hepatocytes. (E) mRNA levels of genes regulating fatty acid transport and synthesis were measured in four groups of primary hepatocytes. * $p < 0.05$, ** $p < 0.01$, *** $p < 0.001$. qRT-PCR: quantitative Real-Time

PCR; TG: triglyceride; TC: total cholesterol; LDL-C: low density lipoprotein cholesterol;
WT: wild-type.

Author Manuscript

Author Manuscript

Author Manuscript

Author Manuscript

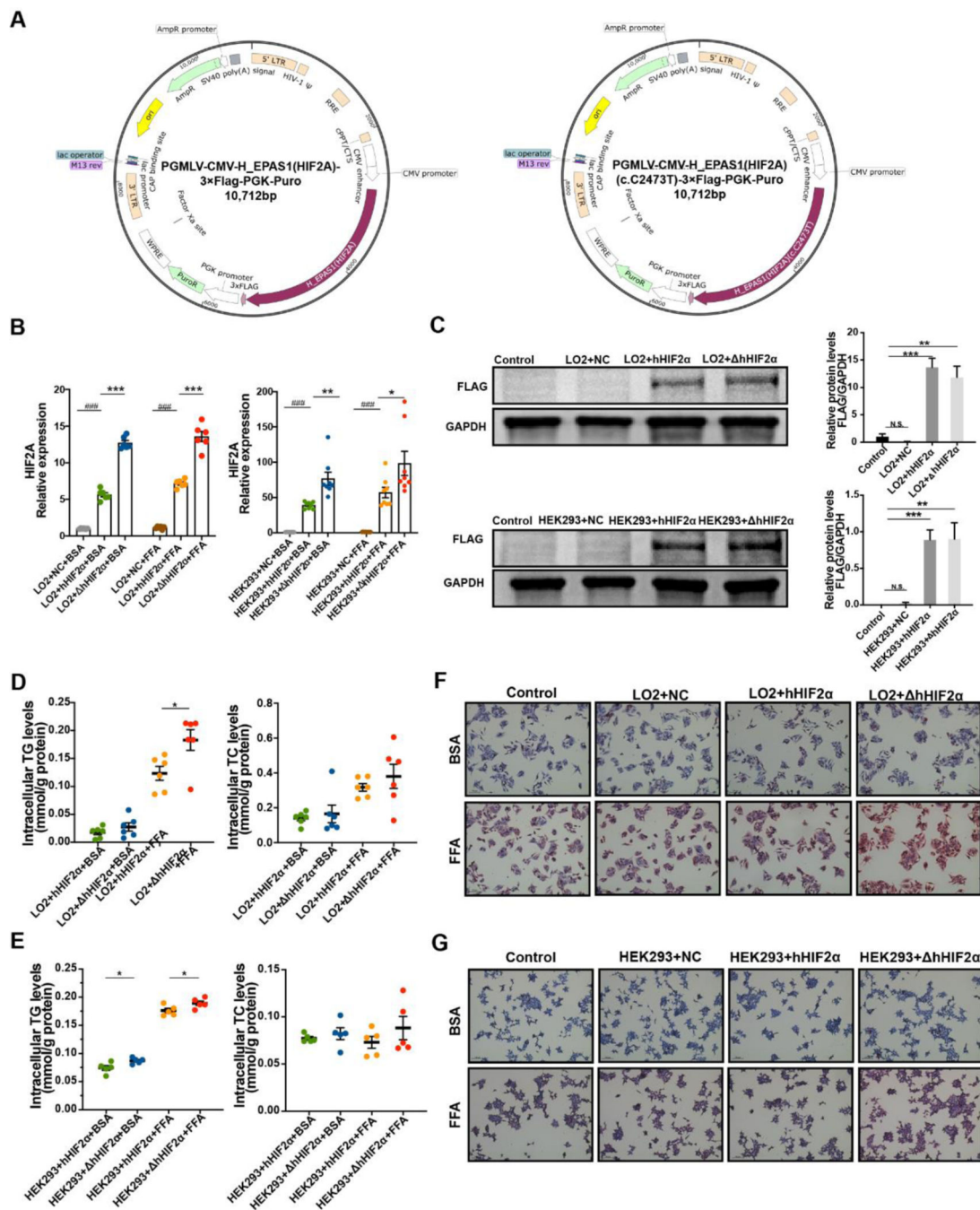


Fig. 5.

Cells lines with HIF-2 α^{mut} were constructed and the mutation caused elevated lipid accumulation. (A) Plasmids with HIF-2 α and HIF-2 α^{mut} were constructed and packaged into lentiviruses. (B) HIF-2 α mRNA levels in LO2 and HEK293 cells. LO2 and HEK293 cells were transfected with NC lentiviruses, lentiviruses with hHIF-2 α , or lentiviruses with hHIF-2 α , and cultured in DMEM containing BSA or FFA, respectively. (C) Protein levels of flag in LO2 and HEK293 cells were assessed by western blot. (D and E) Intracellular TG and TC levels were measured in different treatment groups of LO2 cells (D) and HEK293

cells (E), respectively. (F and G) Oil Red O staining results of LO2 cells (F) and HEK293 cells (G) with different lentiviruses and treatments. * $p < 0.05$, ** $p < 0.01$, *** $p < 0.001$ versus hHIF-2 α group; ### $p < 0.001$ versus NC group. NC: negative control; BSA: bull serum albumin; FFA: free fatty acids.

Author Manuscript

Author Manuscript

Author Manuscript

Author Manuscript

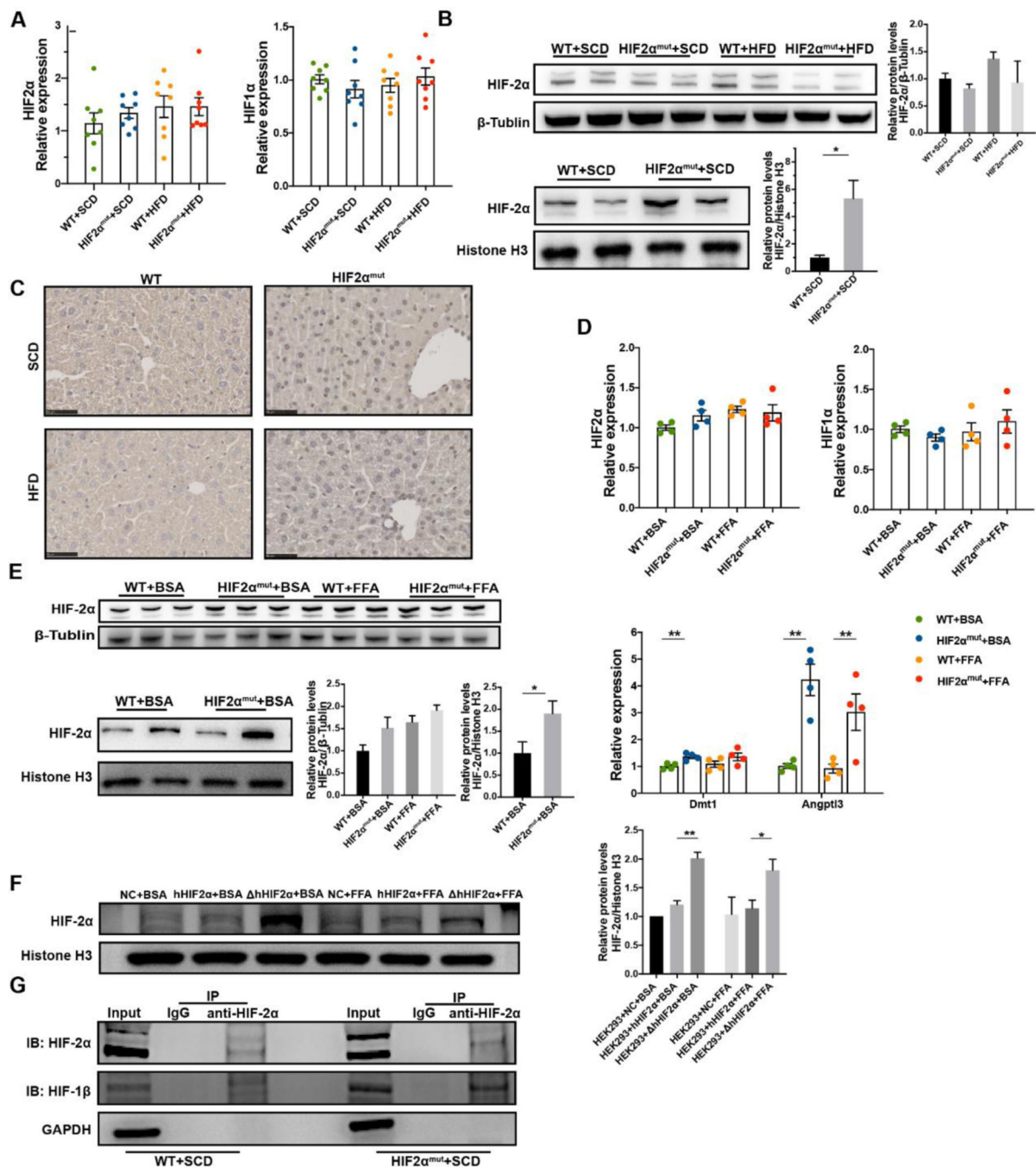


Fig. 6. The mutation increased HIF-2α protein levels in the nucleus. (A) HIF-2α and HIF-1α mRNA levels were assessed by qRT-PCR in WT and mutant mice fed HFD or SCD. (B) Total protein levels of HIF-2α were not significantly different between mutant and WT mice. Nuclear HIF-2α protein levels were elevated in the mutant group. (C) Immunohistochemistry of HIF-2α in mouse liver. HIF-2α^{mut} groups had more stained HIF-2α protein. (D) mRNA levels of HIF-2α, HIF-1α, and the downstream targets of HIF-2α were assessed in primary hepatocytes. (E) Total protein levels of HIF-2α were

similar between mutant and WT primary cells. Nuclear HIF-2 α protein levels were elevated in the mutant group. (F) Western blot showed that the protein levels of nuclear HIF-2 α were elevated in mutant HEK293 cells. (G) Co-immunoprecipitation was performed in SCD-fed HIF-2 α ^{mut} and WT mice. HIF-2 α could bind to HIF-1 β , and mutant HIF-2 α bound more HIF-1 β . * p <0.05, ** p <0.01, *** p <0.001. qRT-PCR: quantitative Real-Time PCR; WT: wild-type; HFD: high-fat diet; SCD: standard chow diet.

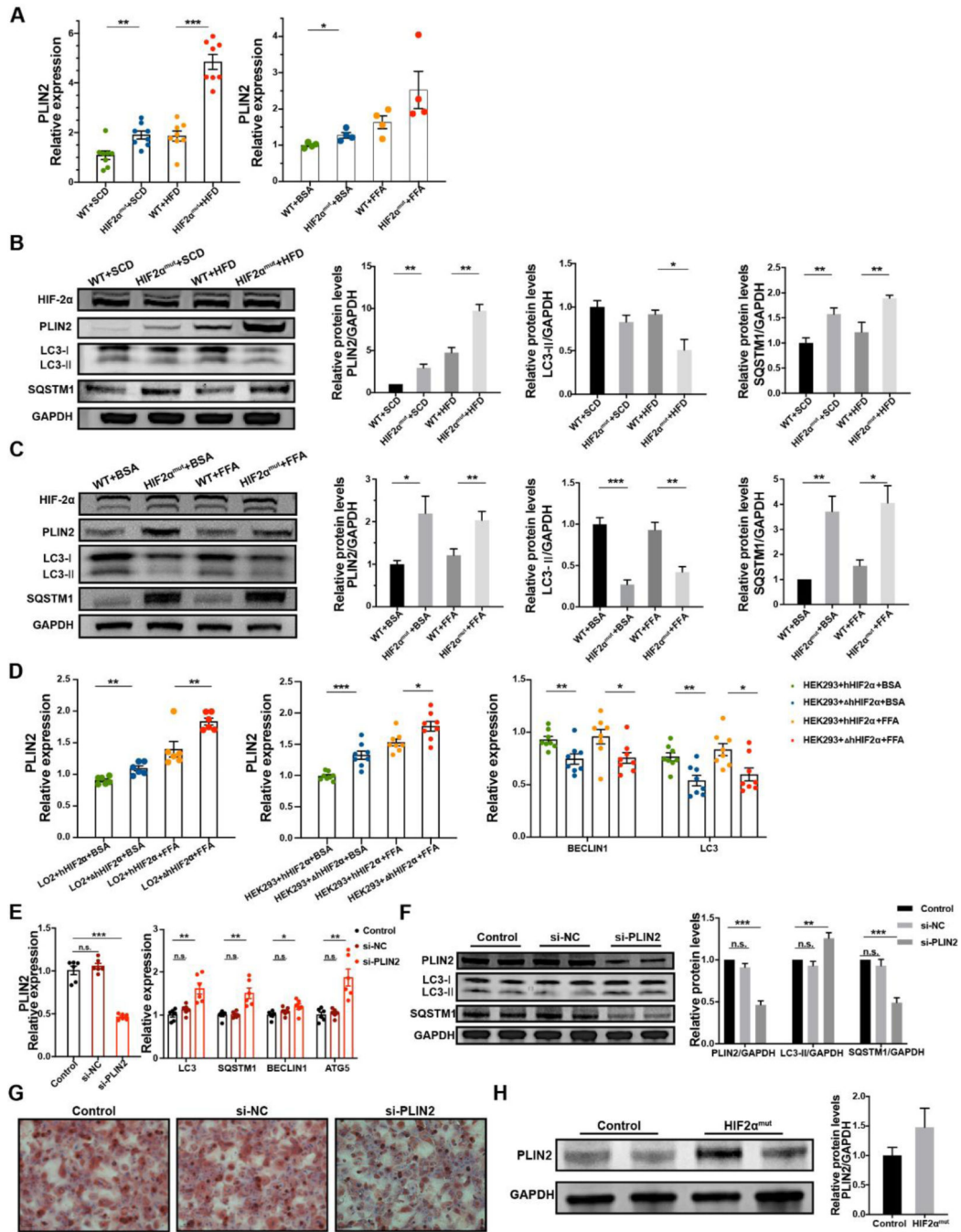


Fig. 7. PLIN2 protects lipid from lipophagy in mutant groups. (A) PLIN2 mRNA levels were compared in mice and primary hepatocytes, respectively. (B and C) Protein levels of HIF-2 α , PLIN2, LC3, SQSTM1 were assessed in mice (B) and primary hepatocytes (C) by western blot. The mutation did not alter HIF-2 α , but elevated PLIN2 and SQSTM1 protein levels and decreased LC3-II/I protein ratio. (D) mRNA levels of PLIN2 were elevated in mutant LO2 and HEK293 cells. Lipophagy-related genes expressed less in mutant HEK293 cells. (E) Primary hepatocytes isolated from mutant mice were as a control. After

transfection of NC or PLIN2 siRNA, mRNA levels of *PLIN2*, *LC3*, *SQSTM1*, *BECLIN1* and *ATG5* in HIF-2 α ^{mut} primary hepatocytes were determined by qRT-PCR. (F) Protein levels of PLIN2, LC3, SQSTM1 were measured in HIF-2 α ^{mut} primary hepatocytes after transfection of PLIN2 siRNA. (G) Oil Red O staining of HIF-2 α ^{mut} primary hepatocytes transfected with NC or PLIN2 siRNA and cultured in DMEM with FFA. PLIN2 siRNA reduced lipid accumulation in mutant primary cells. (H) PLIN2 protein levels in the liver of patients without HIF-2 α ^{mut} (control) and patients with HIF-2 α ^{mut} (patient 4 and 5). * p <0.05, ** p <0.01, *** p <0.001. qRT-PCR: quantitative Real-Time PCR; NC: negative control; FFA: free fatty acids.